Ecology, 94(12), 2013, pp. 2732–2743

On the growth of locally interacting plants: differential equations for the dynamics of spatial moments

Thomas P. Adams,[1,6] E. Penelope Holland,[2] Richard Law,[3] Michael J. Plank,[4] and Michael Raghib[5]

[1]*SAMS, Scottish Marine Institute, Oban, Argyll PA37 1QA Scotland, United Kingdom*
[2]*Landcare Research, P.O. Box 40, Lincoln 7640 New Zealand*
[3]*York Centre for Complex Systems Analysis, Ron Cooke Hub, University of York, York YO10 5GE United Kingdom*
[4]*Department of Mathematics and Statistics, University of Canterbury, Christchurch, New Zealand*
[5]*Ecopetrol–Instituto Colombiano del Petroleo, Km. 7 via Piedecuesta, Bucaramanga, Colombia*

Abstract. Ecologists are faced with the challenge of how to scale up from the activities of individual plants and animals to the macroscopic dynamics of populations and communities. It is especially difficult to do this in communities of plants where the fate of individuals depends on their immediate neighbors rather than an average over a larger region. This has meant that algorithmic, agent-based models are typically used to understand their dynamics, although certain macroscopic models have been developed for neighbor-dependent, birth–death processes. Here we present a macroscopic model that, for the first time, incorporates explicit, gradual, neighbor-dependent plant growth, as a third fundamental process of plant communities. The model is derived from a stochastic, agent-based model, and describes the dynamics of the first and second spatial moments of a multispecies, spatially structured plant community with neighbor-dependent growth, births, and deaths. A simple example shows that strong neighborhood space-filling during tree growth in an even-aged stand of Scots pine is well captured by the spatial-moment model. The space-filling has a spatial signature consistent with that observed in several field studies of forests. Small neighborhoods of interaction, nonuniform spacing of trees, and asymmetric competition all contribute to the buildup of a wide range of tree sizes with some large dominant individuals and many smaller ones.

Key words: individual-based model; Pinus sylvestris; *plant growth; population dynamics; spatial interaction; spatial-moment dynamics; spatial pattern; stochastic model; tree stand development.*

Introduction

The birth, growth, and death of individual plants depend on local environments, especially on interactions with neighbors, rather than on some average state at a large spatial scale. The plant community that we observe is an outcome of past neighborhood processes, and its future depends on how current birth, growth, and death of individuals shape neighborhoods still to come. Recognizing the importance of this, local interactions have been the subject of a great deal of research in plant ecology, particularly in the field of forestry (Canham 1988, Biging and Dobbertin 1992, Canham et al. 2004), including for instance general spatial structure (e.g., Stoyan and Penttinen 2000, Pommerening 2002) and the impacts of shading and other neighborhood processes on recruitment (Barbeito et al. 2008, Tautenhahn et al. 2012).

However, neighborhood processes at a spatial scale relevant to individuals are complex, and this makes it difficult to write down a dynamically sufficient description (sensu Lewontin 1974) of plant community dynamics. As a result, plant ecology now has a rich heritage of individual-based models (IBMs), it being much easier to take a computational approach based on algorithmic rules for behavior of individual plants. Such models are explicitly spatial, and treat individual plants as agents that interact with others in their neighborhood in particular ways. They range from single-species, birth–death processes (Kendall 1948) to multispecies forest gap models such as SORTIE and TROLL, with growth and dispersal fully parameterized for particular communities of interest (Pacala et al. 1996, Chave 1999, Pommerening et al. 2011). These models have made it possible to understand how species characteristics lead to broader scale structure in both a spatial and temporal sense (succession).

The drawback of specialized, stochastic, individual-based models is that they tend to be quite intractable mathematically. Tractable approximation schemes that capture their basic properties are still called for (Gratzer et al. 2004). A scheme based on space-filling by forest trees, for instance, allowed the von Foerster equation (von Foerster 1959) to be used to model successional dynamics of some forest communities (Purves et al. 2008, Strigul et al. 2008). With this, it was possible to scale tree growth up to the landscape level (Bohlman and Pacala 2012) and to global climate and nutrient

Manuscript received 25 January 2013; revised 5 April 2013; accepted 6 May 2013. Corresponding Editor: M. Uriarte.
[6] E-mail: tom.adams@sams.ac.uk

cycling processes (E. Weng et al., *unpublished data*) However, this scheme did not deal with the local scales at which neighbors interact. Finding good macroscopic approximations for the microscopic behavior of agents in IBMs remains a major challenge for ecologists (Levin 2012).

Spatial-moment dynamics are potentially promising schemes for approximation. They have already provided a formal framework for modeling neighborhood dependence of births and deaths (Bolker and Pacala 1997, Dieckmann and Law 2000), and have shown some of the complexities of dynamics that are hidden until spatial structure is taken into account (e.g., Bolker et al. 2003, Law et al. 2003, Murrell and Law 2003). They have also been used to describe the emergence of spatial pattern for a birth–death process of plants that grow from discrete juvenile to adult stages (Murrell 2009). However, these models have not dealt with the gradual growth of individuals and the development of size structure that emerges from this. It is important that they should do so, because plant body size is a key mediator of interactions among neighbors and their resulting resource acquisition (Adams et al. 2007), of reproductive output (Ribbens et al. 1994, Clark et al. 2004), and of the risk of death (Taylor and MacLean 2007).

This article shows how spatial-moment dynamics can be used to scale up from the microscopic interactions among neighboring plants to the macroscopic growth of whole stands. (The Appendix provides a general derivation of a spatial moment dynamical system for a multispecies plant community with birth, growth, and death of locally interacting plants.) As stands develop, they build up size distributions contingent on spatial arrangement and the degree to which competition is asymmetric (Weiner and Damgaard 2006). These size distributions are of special interest in agriculture and forestry, because they determine the yields (Weiner et al. 2001*a*) and hence profits generated. They are also of interest in the transition from commercial to amenity forestry where even-aged stands need to be changed efficiently to size and spatial structures closer to that of natural woodlands (Schutz 2002, Adams et al. 2011*b*). For such applications, an understanding of the relationship between size and spatial structure will bring clear benefits.

Methods

Here we describe the growth of a single-species stand in which plants interact with their neighbors, first as an individual-based stochastic process that encapsulates some basic features of local interactions, and second as a deterministic model derived from the stochastic process (the derivation is given in the Appendix). We focus on growth; this is the most novel part of the birth–death–growth model, and is of interest in its own right because it epitomizes much of agriculture and forestry. Moment approximations for birth–death processes have been described in earlier work (Bolker and Pacala 1997, Dieckmann and Law 2000).

The plants are assumed to live in a large, homogeneous, two-dimensional space, each plant having a center of location given by Cartesian coordinates $x = (x_1, x_2)$ and a size $s = \ln(w/w_0)$, where w_0 is an arbitrary mass. Size is measured on a logarithmic scale because plants often grow over several orders of magnitude in the course of their lives. Thus the state of plant i is given by $(x, s)_i$ and the state p of the stand as a whole is made up of the locations and sizes of all the plants it contains, i.e., $p = \{(x, s)_1, (x, s)_2, \ldots\}$.

Stochastic model

We define a growth rule for plants that grow in small steps δs. For a stand at state p, the probability of plant i making a size increment δs over a short period of time δt is $\hat{G}_i(p)\delta t/\delta s$, where $\hat{G}_i(p)$ is given by

$$\hat{G}_i(p) = g(s_i) + g' \sum_{j \neq i} w\Big((x, s)_i, (x, s)_j\Big) \qquad (1)$$

if $\hat{G}_i(p) \geq 0$, and zero otherwise, to ensure that plants cannot shrink. This is a Poisson process with rate $\hat{G}_i(p)/\delta s$. The term $g(\cdot)$ is a relative growth rate that plant i would have in the absence of competition (e.g., Gompertz); $w(\cdot)$ is a competition kernel describing the effect of a neighbor plant j on the growth of the target plant i; g' is a negative quantity with dimensions time^{-1} that scales the strength of neighborhood effects; the summation is over all neighbor plants (referred to as a "shot-noise field" by Illian et al. [2008], Pommerening et al. [2011]). At this stage, the competition kernel does not need to be specified. Nevertheless, the assumption of a homogeneous environment can be incorporated at this point by replacing physical locations of the plants with the displacements between plants in two dimensions $\boldsymbol{\xi} = (\xi_1, \xi_2)$. Isotropy is also assumed, but we keep the two Cartesian dimensions as this helps to understand the geometries (Fig. 1). In the continuous space–size moment approximations that follow, the competition kernel is then written as $w(\boldsymbol{\xi}', s, s')$, where $\boldsymbol{\xi}'$ is the displacement from the target to the neighbor, s is the target size, and s' is the neighbor size.

The number of growth events $N_i(T)$ experienced by plant i over a period of time T is a Poisson random variable with mean $\int_0^T (\hat{G}_i(p(t))/\delta s)dt$ (Grimmett and Stirzaker 2001). The increase in size of plant i over this time is $S_i(T) = N_i(T)\delta s$, which is a random variable with mean $M(T) = \int_0^T \hat{G}_i(p(t))dt$ and variance $M(T)\delta s$. Therefore, the ratio of variance in size to mean size is equal to δs. It is realistic to expect some variability in size to develop, even among plants that experience identical levels of competition. δs is a model parameter that allows the level of variability to be set, without substantially altering the mean growth rate, as shown in Appendix Fig. A.3. In the limit $\delta s \to 0$, plant growth effectively becomes deterministic, with growth rate $dS_i/dt = \hat{G}_i(p(t))$.

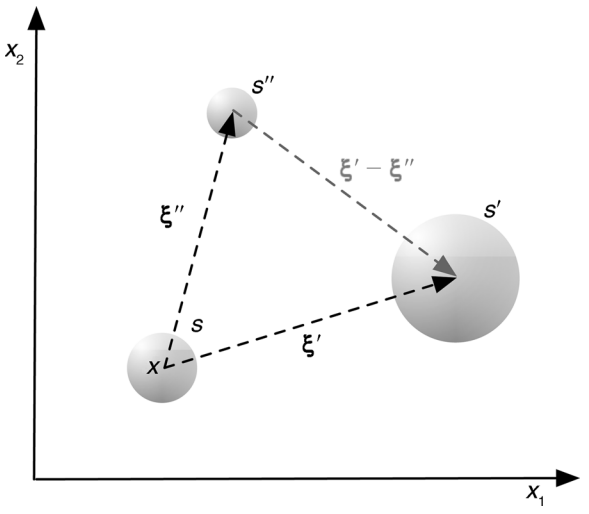

FIG. 1. Vector separations (ξ) between individuals of different sizes (s denotes log-transformed size of plants).

Spatial moments

Statistical measures of spatial structure describing the outcome of a stochastic process on a population of individuals can be more instructive than attempting to interpret the complex output from multiple realizations of the stochastic process itself. Moreover, these measures become the variables of the macroscopic approximation.

The first three spatial moments (defined formally in the Appendix) are as follows, with notation for displacements and sizes as in Fig. 1. These moments change over time as the plants grow, so they have time t as an argument. The first moment $m_1(s, t)$ is the density of individuals of size s at time t. This function is familiar in ecology as the size distribution of individuals. Crucially, it carries no information about how plants of different sizes are distributed in space and is insufficient for modeling growth dynamics of plants interacting in neighborhoods. The second spatial moment $m_2(\xi', s, s', t)$ is the density of pairs of individuals with size s and s' at time t, the s' individual being displaced by a vector ξ' from s. This moment is more intricate, describing the density of all combinations of pairs of sizes at all displacements, and plays a key part in this paper, as it holds all the second-order, space–size information in the stand. The third spatial moment $m_3(\xi', \xi'', s, s', s'', t)$ goes a step further to the density of triplets of individuals with size s, s', and s'', the s' individual being displaced by a vector ξ' from s and the s'' individual displaced by a vector ξ'' from s.

Although the dynamics that follow are built on the pair density, this measure has too many dimensions for easy visualization. Some of the basic space–size properties that develop as a stand grows are better seen in terms of the mark pair density, and especially in terms of its related mark correlation function (Stoyan and Penttinen 2000, Illian et al. 2008, Suzuki et al. 2008, Law et al. 2009). The mark pair density function takes the product of the sizes in each pair, thereby reducing the number of arguments in the pair density from four to two (see Appendix A1.2). The mark correlation function is a normalization of the mark pair density that measures the residual spatial organization of mass pairs after removing the spatial structure due to the locations of the plants in space. Consider, for instance, a spatial pattern in which plants are aggregated. If plant sizes are independent of this aggregation, the mark correlation function returns a value close to 1.0 at all distances. However, if the sizes of pairs are positively (respectively, negatively) correlated at some distance, the function returns a value greater (respectively, less) than 1.0 at this distance. Low values of the mark correlation function at short distances are therefore a signature of biomass being distributed more uniformly over space than the plant locations (and high values would be a signature of biomass being even more clustered than the plant locations).

Moment dynamics

The dynamics of the first two spatial moments are derived for growth, birth, and death processes of multiple species in the Appendix. In the case of a single species and growth only, the dynamics are:

$$\frac{\partial m_1}{\partial t} = -\frac{\partial [m_1 G_1]}{\partial s} \tag{2}$$

$$\frac{\partial m_2}{\partial t} = -\frac{\partial [m_2 G_2]}{\partial s} - \frac{\partial [m_2 G_2']}{\partial s'} \tag{3}$$

in the limit as $\delta s, \delta t \to 0$. In writing Eq. 3, a symmetry $m_2(\xi', s, s') = m_2(-\xi', s', s)$ has been used; in other words, the density of the pair is the same for s and s' with displacement ξ' as it is for s' and s with displacement $-\xi'$. The arguments have been suppressed for clarity here; in full they are: $m_1(s, t)$, $G_1(s, t)$, $m_2(\xi', s, s', t)$, $G_2(\xi', s, s', t)$, where G_2' denotes $G_2(-\xi', s', s, t)$. Note that, when $\delta s > 0$, the dynamics are described by the discretized form of Eqs. 2 and 3, with a step size of δs (see Appendix Eq. A.17). This is worth highlighting because, ordinarily, the differential equation is the accurate description and the discretized form is a numerical approximation. Here, the discretized form is the accurate description for the average of the stochastic model when $\delta s > 0$, as illustrated in Appendix Fig. A.3.

Eq. 2 is similar to a size-based version of the McKendrick-von Foerster equation, by assumption without mortality here (von Foerster 1959, Sinko and Streifer 1967, Silvert and Platt 1978, Strigul et al. 2008). The flux terms of Eq. 3 are similar, except that there are now two terms to deal with growth of a pair. The growth rates themselves are:

$$G_1(s,t) = g(s) + g' \iint w(\xi', s, s') \frac{m_2(\xi', s, s', t)}{m_1(s,t)} d\xi' ds' \tag{4}$$

$$G_2(\xi', s, s', t) = g(s) + g' \iint w(\xi'', s, s'') \frac{m_3(\xi', \xi'', s, s', s'', t)}{m_2(\xi', s, s', t)} d\xi'' ds'' + g' w(\xi', s, s') \tag{5}$$

where $g(s)$, $w(\xi', s, s')$, and g' are as defined following Eq. 1. The denominators in these equations follow from the rules of conditional probability as shown in the Appendix. As in the stochastic model, the growth rates are replaced with zero if they become negative, ensuring that, on average, the plants cannot shrink (this is not precisely the same as the assumption in the stochastic model; see *Discussion*). The integrals add up the effect of neighbors on the growth rate, weighting a density by the appropriate value from the competition kernel. The final term in G_2 allows for competition with the other individual in the pair.

Notice that Eqs. 2 and 3 are coupled hierarchically. The dynamics of the first moment in Eq. 2 depend on the second moment m_2 in Eq. 4, which has the consequence that the size distribution that unfolds over time depends on the spatial structure. Similarly, the dynamics of the second moment in Eq. 3 depend on the third moment m_3 in Eq. 5. This hierarchical structure is typical of spatial moment dynamics. For practical purposes, the hierarchy does need to be closed at some level, replacing the next moment by some function of lower-order moments. Historically, ecologists have usually closed the hierarchy at first order using a mean-field assumption, thereby ignoring all spatial information. In this paper we close the hierarchy at second order to retain some basic information on spatial structure, extending a so-called asymmetric, power-2 closure previously found to work well under a wide range of spatial structures for the logistic equation (Murrell et al. 2004):

$$\hat{m}_3(\xi', \xi'', s, s', s'') = \frac{1}{q_1 + q_3} \left(q_1 \frac{m_2(\xi', s, s') m_2(\xi'', s, s'')}{m_1(s)} + q_2 \frac{m_2(\xi', s, s') m_2(\xi'' - \xi', s', s'')}{m_1(s')} + q_3 \frac{m_2(\xi'', s, s'') m_2(\xi'' - \xi', s', s'')}{m_1(s'')} - q_2 m_1(s) m_1(s') m_1(s'') \right) \tag{6}$$

if $\hat{m}_3(\xi', \xi'', s, s', s'') \geq 0$, and 0 otherwise, and with weighting on the three corners $q_1 = 4$, $q_2 = 1$, $q_3 = 1$. The time argument has been omitted from all functions here for simplicity.

Numerical methods

How useful the deterministic approximation (Eqs. 2 and 3) is in practice depends on whether it provides an acceptable approximation for the ensemble behavior of plants growing together in a stand. The yardstick for this is the stochastic process, and the comparison is a numerical matter that needs explicit functions for growth with given parameter values. We used the functions that follow to do this, taking parameter values appropriate for growth of Scots pine (*Pinus sylvestris*; see Plate 1) trees (derived from those of Adams et al. 2011*a*).

The Gompertz equation was taken as the basis for intrinsic growth of the trees, as follows:

$$g(s) = \alpha - \beta s \tag{7}$$

with two parameters, α being the intrinsic relative growth rate at small size, and β representing how much growth decreases with increasing size; the ratio α/β gives the asymptotic size to which a tree grows, i.e., the size at which the relative growth rate becomes zero. The Gompertz function sits within the Richards (1959) family of growth models, and several studies have found it to be the best descriptor of plant growth for species investigated (Zeide 1993, Purves and Law 2002, Schneider et al. 2006, Adams 2010).

We took a simple form of the competition kernel, separating it into three parts for the effect of a neighbor on a target (Fig. 2). Firstly, this incorporated the sizes of the trees, on the grounds that competition would be stronger the larger the trees are. Second, we assumed an asymmetry such that larger trees would have a more deleterious effect on smaller trees than vice versa, using a tanh function for the purpose (Fig. 2a). Third, we used a Gaussian function for the distance between the trees, on the grounds that competition would become weaker the greater the separation of the trees (Fig. 2b). Bringing these components together gives

$$w(\xi', s, s') = (s + s') \times [1 + \tanh(\gamma(s' - s))] \frac{1}{W} \exp\left(-\frac{|\xi'|^2}{2\sigma^2} \right). \tag{8}$$

Here $|\xi'|$ is the distance from the target to the neighbor, the parameter σ sets the spatial range of interactions, and the nonnegative γ measures the degree to which competition is asymmetric (taking a value of zero when there is no asymmetry). The Gaussian function was truncated at 3σ, and normalized to integrate to 1, $1/W$ being the normalization factor. Truncation is needed for stochastic simulations in a finite arena with periodic boundaries to ensure that neighbors cannot be counted more than once; for consistency the same truncation was used in the deterministic model.

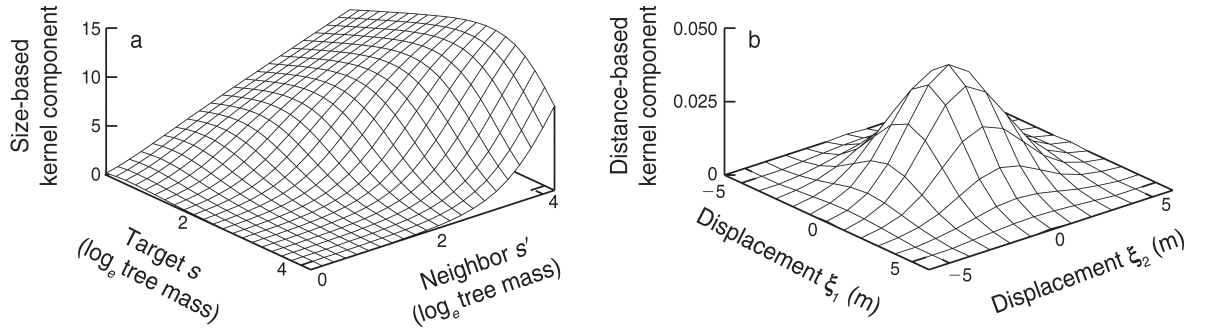

FIG. 2. Components of the competition kernel, $w(\xi, s, s')$, Eq. 8, where s is a measure of tree size, and ξ is the displacement between trees. (a) Effect of neighbor tree of size s'' on target of size s (with $\gamma = 1$, where γ measures the degree to which competition is asymmetric). Size is $\log_e$-transformed tree mass. (b) Effect of neighbor displaced in two dimensions by $\xi = (\xi_1, \xi_2)$ on the target tree at the origin (with $\sigma = 2$ m, where σ sets the spatial range of interactions).

Therefore there are six parameters in the growth model, together with the step size for growth δs, a time step δt, and spatial displacement steps $\delta\xi_1$, $\delta\xi_2$ for discretization of the continuous moment model for numerical integration (Table 1). The step size for growth, δs, is used here as a parameter to set the intrinsic variability in body size that develops as the trees grow. Some variation in growth is almost certain to arise for developmental and genetic reasons; the limit as $\delta s \to 0$ in Eqs. 2 and 3 represents a special case. For consistency, numerical analysis of the stochastic and deterministic models must use the same value of δs.

The high dimensionality of the second moment, with two size dimensions and two displacement dimensions, requires some compromises so that it does not become too large in its discretized vector form for integration to be feasible. Tree growth was therefore started at 10 kg (corresponding to $s = 0$). Our Gompertz growth parameters were obtained by converting growth of "diameter at breast height" (found by Adams [2010] to reach an average asymptote of 62.9 cm, with substantial variation between individuals) to growth of aboveground biomass [Eq. 347 of Zianis et al. 2005). These parameters give a maximum individual tree size of 4.2 on the log mass scale (~700 kg), this being almost entirely achieved by about 200 years. We used a fairly coarse spatial binning, so that overall the discretized second moment would have at most around 60 000 elements. Using a finer spatial binning does not have a notable impact on the results, but may be useful if a particularly fine definition spatial signature is required. Parameter values used in the numerical analysis are given in Tables 1 and 2.

Realizations of the stochastic process (Eq. 1) were computed using the Gillespie algorithm (Gillespie 1977) for a stand at some initial state p_0 in an arena of size 50 × 50 m with periodic boundaries. The density was set at 0.25 trees/m^2, i.e., 625 trees, corresponding to the 2-m lattice average density used in Scots pine plantations in the United Kingdom (Mason 2000). Initial sizes were allocated to the trees independently and uniformly in the range $0 \le s \le 0.2$, so that all started at approximately the same size. Spatial patterns were constructed as Poisson, aggregated, or inhibited as required; non-Poisson patterns were obtained by moving points at random in the arena to minimize the deviation from a chosen pair correlation function $c_2(|\xi|)$. We used an exponential function, $c_2(|\xi|) = 1 + (c_{2,0} - 1)e^{-c|\xi|}$ for the purpose; with increasing distance $|\xi|$, this decays to 1 with a rate constant c, starting from an initial value $c_{2,0}$. Here $c_{2,0} > 1$ gives local aggregation of plants in space, $c_{2,0} < 1$ gives local inhibition, and $c_{2,0} = 1$ gives a Poisson pattern lacking spatial structure. Plants were assumed to stay at the same location throughout the period of stand development, and the spatial pattern of points was therefore fixed at its initial state. However, the spatial pattern of plant sizes was free to change during the growth of the plants, as allowed by neighborhood competition. The stochastic realizations returned the state p over time, from which the spatial moments could be computed to compare with the deterministic model. An average over 10 realizations was used for the comparison and gives a sufficient

TABLE 1. Parameters for modeling growth of a stand of Scots pine, with values for those held constant throughout.

Symbol	Value	Units	Definition
α	0.0634	yr^{-1}	intrinsic relative growth rate when small
β	0.0149	yr^{-1}	size-dependent decline in growth
g'		yr^{-1}	strength of competition
γ			strength of asymmetry
σ		m	spatial range of interactions
w_0	10	kg	aboveground biomass at which $s = 0$
δt	0.1	yr	step size for time
δs	0.2		step size for growth
$\delta\xi_1$, $\delta\xi_2$		m	step size for spatial displacements ξ_1, ξ_2
ξ_{max}		m	maximum displacement for computing $m_2(\xi, s, s', t)$

TABLE 2. Parameters taking more than one value in numerical results, as depicted in the figures.

Figure	g'	γ	σ	ξ_{max}	$\delta\xi_1$, $\delta\xi_2$	Spatial pattern	
						$c_{2,0}$	c
3a	0.04	0.0	10.0			3.0	0.5
3b	0.04	0.0	2.0			3.0	0.5
3c	0.04	1.0	2.0			3.0	0.5
4a	0.0			30.0	3.0	1.0	0.0
4b	0.04	0.0	10.0	30.0	3.0	1.0	0.0
4c	0.04	1.0	2.0	12.0	1.0	3.0	0.5
5a, b light	0.04	0.0	10.0	30.0	3.0	3.0	0.5
5a, b dark	0.04	0.0	2.0	12.0	1.0	3.0	0.5
5c, d light	0.04	0.0	2.0	12.0	1.0	0.3333	0.5
5c, d dark	0.04	0.0	2.0	12.0	1.0	3.0	0.5
5e, f light	0.04	0.0	2.0	12.0	1.0	0.3333	0.5
5e, f dark	0.04	1.0	2.0	12.0	1.0	0.3333	0.5

Note: Spatial pattern is defined by a function $c_2(|\xi|) = 1 + (c_{2,0} - 1)e^{-c|\xi|}$, where $c_{2,0}$ sets the initial level of spatial aggregation and c is the rate constant.

population size for average behavior to be well defined (a total of 6250 individuals).

The deterministic model was solved by numerical integration using the Euler method on Eq. 3, discretized in plant size, spatial displacement, and time. A time step $\delta t = 0.1$ was used, which ensures that the required stability criterion ($g(\cdot)\delta t/\delta s \leq 1$; Adams 2010) is always satisfied. It is sufficient just to use Eq. 3 for the integration, because $m_2(\xi, s, s', t) = m_1(s, t) \times m_1(s', t)$ for large enough ξ_1 and ξ_2, denoted ξ_{max}; in other words, the size distribution is known from the boundary of the second moment. The initial condition for $m_2(\xi, s, s', t)$ was set to match the initial state of the corresponding second moment of the stochastic model. The third moment was eliminated from Eq. 3 using a power-2 closure with a 4, 1, 1 weighting on the s, s', s'' corners, as described in Eq. 6.

RESULTS

Stochastic model: growth with neighborhood competition

The spatial pattern of tree growth depends very much on the action of local competition. We illustrate this using three realizations of the stochastic process, with the trees distributed in a fixed, aggregated spatial pattern (Fig. 3a–c). Large differences among these three stands are clearly evident after 150 years, even though the realizations had exactly the same aggregated pattern in space (see Fig. 3d for the pair correlation function), and exactly the same initial tree size at each location. Individuals in the first example (Fig. 3a) had a large interaction neighborhood. This means that inhibition of growth of all trees was close to the mean-field value, i.e., determined by the spatial average density, so all trees grew to a similar intermediate size regardless of their spatial location (Fig. 3e). In contrast, the second example assumed a small neighborhood, meaning that the number of neighbors varied greatly from tree to tree, and trees with few neighbors were much larger after 150 years than trees with many neighbors (Fig. 3b, e). In Fig. 3a and b, interactions between individuals were symmetric: there was no advantage to being larger. Breaking the symmetry, so that bigger individuals gained an advantage in competition, increased the variability in size still further, a small proportion escaping from competition and becoming especially large, leading to a slightly bimodal size distribution (Fig. 3c, e).

The most important feature, however, is the far from random spatial pattern of tree sizes, given the locations of trees, evident in Fig. 3b and c. In Fig. 3b, large individuals tend to be in gaps where they have a small number of neighbors; in Fig. 3c, large individuals are additionally seen in the clusters, where they are surrounded by small individuals that they have suppressed. The mark correlation functions (Fig. 3f) summarize this spatial information in a precise way. In realization (a), the mark correlation function computed from the space–size pattern is close to unity, there being little spatial structure in tree size to be accounted for after allowing for the aggregated spatial pattern. In realization (b), however, the mark correlation function is substantially less than 1.0 at short distances, indicating that mass is distributed much more uniformly across space than the locations of the trees. The local inhibition of mass is still stronger in the presence of asymmetric competition, in realization (c).

It is this spatial, neighborhood-dependent growth that lies at the heart of stand development, and it is this process that the moment dynamics attempt to capture.

Comparison of stochastic and moment models

To test how well the deterministic approximation (Eq. 3) works, Fig. 4 compares solutions of the spatial-moment model with those of the stochastic model over a range of behaviors.

The most basic case is that of independent trees, which experience no competition from neighbors (i.e., $g' = 0$, Fig. 4a). Here tree growth follows the intrinsic path of the Gompertz equation, with some variation generated by the jumps in size δs, and the trees are near to the maximum size allowed by Gompertz growth by 150 years. The distributions in tree size generated by the

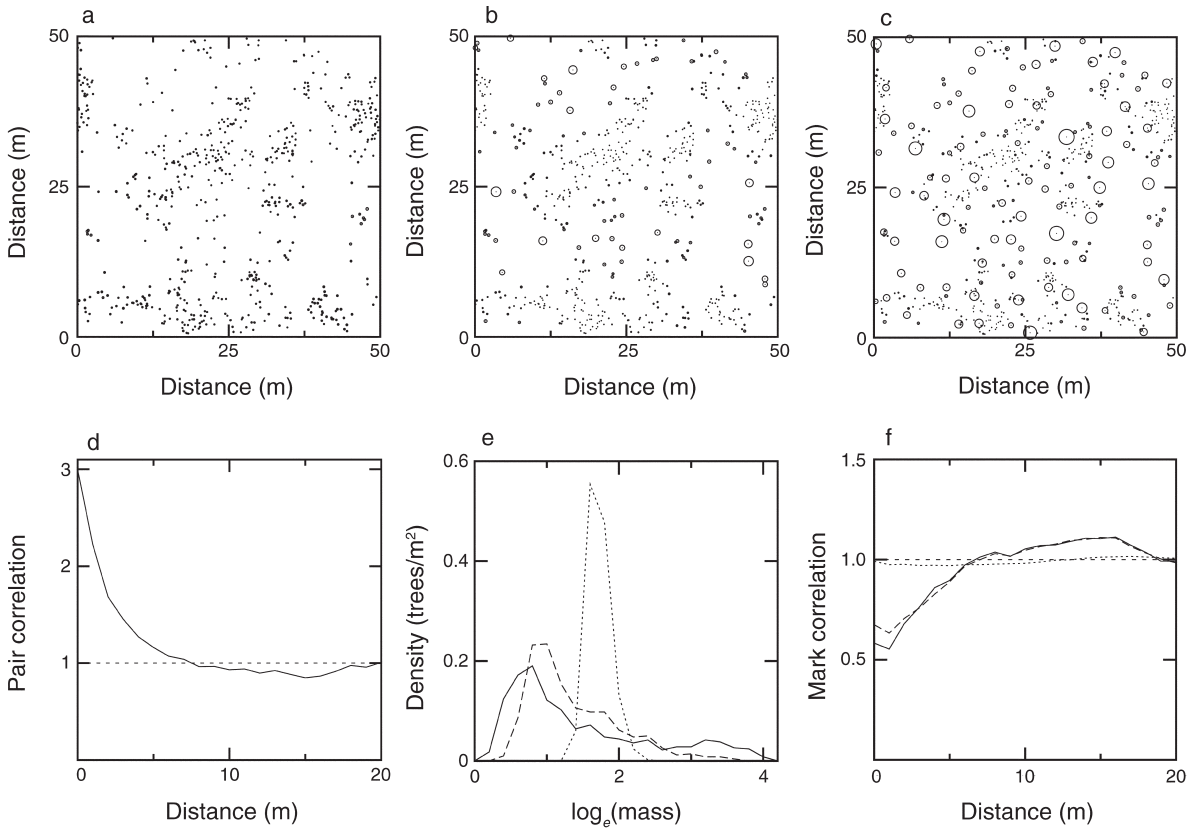

FIG. 3. Stands of trees generated by the stochastic process (Eq. 1) under different kinds of interaction. All realizations use the same aggregated spatial pattern and initial sizes; circle diameter is proportional to untransformed tree mass in year 150. (a) Symmetric competition in large neighborhoods ($\gamma = 0$, $\sigma = 10$ m). (b) Symmetric competition in small neighborhoods ($\gamma = 0$, $\sigma = 2$ m). (c) Asymmetric competition in small neighborhoods ($\gamma = 1$, $\sigma = 2$ m). (d) Pair correlation function for spatial pattern of tree locations. (e) Size distribution for the three stands: the dotted line represents the stand in panel (a); the dashed line represents the stand in panel (b); the solid line represents the stand in panel (c). (f) Mark correlation functions, with line types as in panel (e). Parameter values are as in Tables 1 and 2.

stochastic model and its deterministic approximation remain very similar as they grow, as long as the same size step δs is implemented (Appendix Fig. A.3).

Adding symmetric competition in large neighborhoods (with trees arranged in an unstructured Poisson spatial pattern) leads to major suppression of growth (Fig. 4b). However, large neighborhoods smooth out local variations, so different trees experience a similar amount of competition, and all become stunted to a similar degree (see Fig. 3a). These results are close to those that would be observed from a mean-field model of the dynamics that ignores spatial structure of tree size. The deterministic model remains a close approximation of the stochastic process.

The mean-field behavior contrasts with that in Fig. 4c, where (1) neighborhoods are small, (2) the number of competitors within neighborhoods is highly variable due to the presence of an aggregated spatial pattern, and (3) competition is asymmetric, giving large individuals an advantage over small ones. In this case, some trees escape competition and grow large, while others are suppressed, with the result that much more variation in tree size develops over time (see Fig. 3c). The contrast between this and the mean-field behavior of Fig. 4b illustrates how important it is to deal properly with neighborhoods when competition is local. The moment approximation is clearly not perfect, as it allows rather more growth at intermediate sizes than the stochastic process does. However, it does capture the basic features of stand development seen in the stochastic model, including the effect of spatial structure.

Multiple causes of variable tree size

Broadly, three forces generate a wide range of tree sizes as a stand develops (Fig. 5a, c, e): small neighborhood size (Fig. 5a), spatial aggregation of trees (Fig. 5c), and asymmetric competition (Fig. 5e). These all operate by increasing the heterogeneity among neighborhoods. In the case of small neighborhood size and spatial aggregation, some external heterogeneity exists from the start, and this is enhanced as the trees grow to different extents in their variable neighborhoods. In the case of asymmetric competition, external heterogeneity is not needed; it is enough to have small random jumps in size

causing some trees to become larger than others (and equivalently, to spread out the sizes in the solution of the moment dynamics). Once symmetry is broken, the process snowballs, always giving larger trees an advantage. Just how the size distribution develops is a complex interplay of neighborhood size, spatial pattern, and the strength of the asymmetry in competition.

Note that the mark correlation functions are less than 1.0 at short displacements, if the spatial locations of trees are set to be aggregated (Fig. 5b, d). This is the signature that biomass has become more uniformly distributed over space than the trees themselves during the growth of the stand. In mechanistic terms, it is simply a consequence of trees growing to fill the available space: where there are gaps, the trees grow larger. Notice also that the signature vanishes when the trees grow in a uniform spatial pattern (Fig. 5f). It is still possible for a wide range of tree sizes to develop if competition is sufficiently asymmetric, but the distribution of sizes over space is no longer more uniform than the locations of the trees themselves.

Discussion

Evidently the microscopic, stochastic, agent-based model for growth of locally interacting plants can be reduced to a parsimonious dynamical system describing the growth of whole stands. The step from the stochastic to the deterministic model separates the average behavior from the stochastic fluctuations that are inherent in realizations of the stochastic process, and contributes to the goal of scaling up from agent-based models to macroscopic approximations (Levin 2012). The equations themselves provide mathematical insight into the mechanisms at work in the IBM, these being simple advection processes in Eqs. 2 and 3, determined by growth rates that depend on population structure via the spatial moments (Eqs. 4 and 5). In the context of purely deterministic models, the step from the mean field, von Foerster model to a model with local interactions, as used here, is essentially a straightforward matter of going from the first moment to the second (spatial) moment.

The results point to the richness in dynamics of stand growth uncovered by removing the mean-field assumption. Nonetheless, the study does no more than scratch the surface of potential applications, as it deals only with the growth of an even-aged, single-species stand of plants, without births and deaths. The potential for analysis of the dynamics of birth–growth–death processes of multispecies plant communities is an interesting challenge for further work, and can be built on the foundations given in the Appendix. With births and deaths, as well as growth, the spatial patterns will unfold in different ways over time, depending on the kernels for seed dispersal and neighborhood-dependent births and deaths, giving much richer dynamics. The study here, and previous ones of moment dynamics, identify neighborhood interaction kernels as key functions about

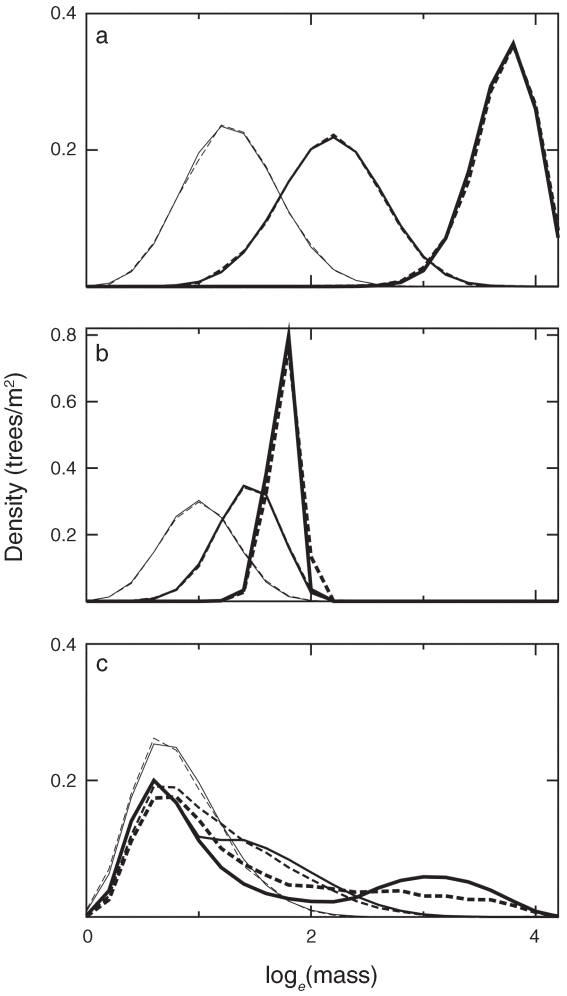

Fig. 4. Comparison of spatial-moment approximation (Eq. 3) and stochastic model (Eq. 1). (a) Independent trees ($g' = 0$, where g' is strength of competition). (b) Poisson distributed trees competing symmetrically in large neighborhoods ($g' = 0.04$, $\gamma = 0$, $\sigma = 10$ m). (c) Aggregated trees competing asymmetrically in small neighborhoods ($g' = 0.04$, $\gamma = 1$, $\sigma = 2$ m). Average stochastic (dashed) and deterministic (solid) size distributions are superimposed at 25, 50, and 150 years with increasingly heavy lines with time. Parameter values are as in Tables 1 and 2.

which much more needs to be known (Schneider et al. 2006), despite the difficulties involved in the field (Biging and Dobbertin 1995, Canham et al. 2004).

In numerical terms, the spatial-moment approximation captures the broad properties of the stochastic behavior of individual agents, but it is by no means perfect. To some extent we think this is due to the rather coarse discretization of the second spatial moment needed to keep the computations feasible. Because the spatial moments are radially symmetric, it could help to move from a Cartesian to a radial version of the second moment. This would reduce the number of dimensions of the problem, allowing a finer spatial discretization to be used. However, the deterministic approximation does

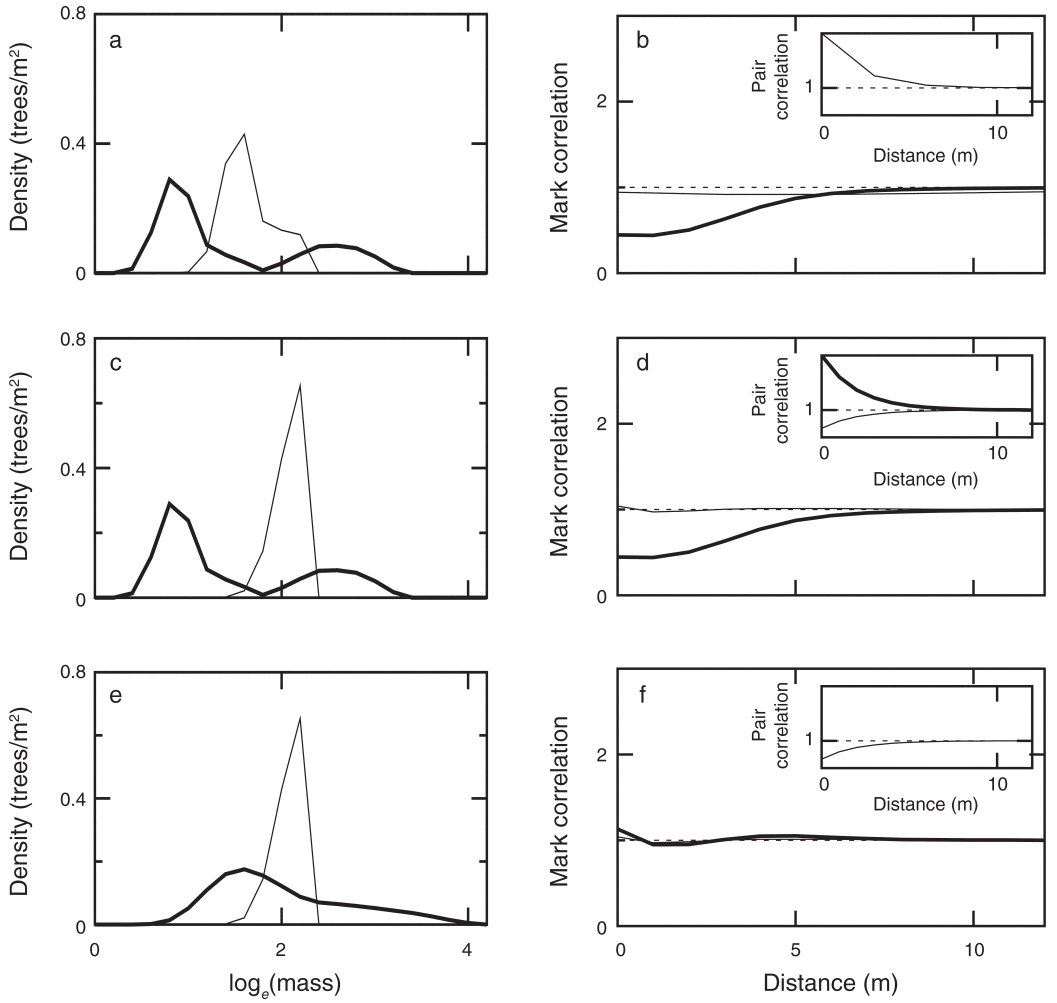

FIG. 5. Three ways to obtain wide size distributions; results are given after 150 years of tree growth using the deterministic approximation (Eq. 3). Size distributions are shown in the left-hand panels; right-hand panels shows mark correlation functions, with pair correlation functions as insets. (a, b) Decreasing neighborhood size from large (light lines, $\sigma = 10$ m) to small (heavy lines, $\sigma = 2$ m) in an aggregated spatial pattern. (c, d) Changing spatial pattern from inhibited (light lines, $c_{2,0} = 1/3$) to aggregated (heavy lines, $c_{2,0} = 3$). (e, f) Increasing asymmetry from 0 (light lines, $\gamma = 0$) to 1 (heavy lines, $\gamma = 1$) in an inhibited spatial pattern. Parameter are values as in Tables 1 and 2.

become less good as the departure from mean field becomes large, and as the degree of asymmetric competition becomes large. We therefore caution users that there are likely to be parameter settings too far from mean field for the approximation scheme to be reliable. Another possible cause of discrepancy is that the assumption of nonnegative growth applies at the level of the individual in the stochastic model and at the level of the average in the deterministic model. As a result, the deterministic model may underestimate the average growth when neighborhood competition becomes intense. It would be necessary to go deeper into the variance of competition to allow for this truncation in the distribution of neighborhood competition. The closure function itself may introduce some error. We used an asymmetric power-2 closure that previously has been found to work well (Murrell et al. 2004) and, consistent with the earlier work, our tests found this to give a closer approximation to the stochastic process than a fully asymmetric power-2 closure. However, it would be instructive to compare this with other closures such as the maximum entropy closure suggested by Raghib et al. (2011). A closure at least at second order is definitely needed: the results show clearly that a first-order, mean-field closure would be seriously misleading when interactions are local in space.

The discretization of body size in steps of δs plays a special role in the two models, and was kept as a free parameter to control how much intrinsic variation in body size develops, in addition to variation generated by interactions among plants. Some variation of this kind is almost certainly bound to be present as, even under the most carefully controlled conditions, plants do not grow at exactly the same rate. It is important to understand

PLATE 1. Mixed-age stand of Scots pine (*Pinus sylvestris*) above Gleann Sheileach, Argyll, Scotland. Photo: T. P. Adams.

that the spatial-moment dynamics given in Eqs. 2 and 3 represent a special case at which $\delta s \to 0$, meaning that such variation is absent. There are other ways of incorporating variation in the continuous growth model, for instance, through the presence of a diffusion term (Datta et al. 2010) that would also be worth considering.

A key ecological property of the results is the tendency for space-filling to take place during plant growth. In qualitative terms, there is no surprise about this, and it has been taken as axiomatic for modeling dynamics of tree canopies (Purves et al. 2008, Strigul et al. 2008). The results here add quantitative knowledge about the path of space-filling, and the degree to which it contributes spatial structure to the community. Spatial patterns that are random or aggregated clearly leave more scope for space to be filled than patterns with local inhibition of individuals, as long as neighborhoods are sufficiently small. Asymmetric competition also generates space for further growth of larger plants, but it does so in a more cryptic way through the larger plants suppressing the smaller ones.

Space-filling leaves a clear signal in the spatial organization of biomass, giving the mark correlation function a characteristic signature that is low at short distances, increasing to a value close to 1.0 as distance increases (Stoyan and Penttinen 2000, Law et al. 2009). Mark correlation functions have rarely been studied in forests. In the small number of studies we know of, such space-filling has been observed in several cases (Penttinen et al. 1992, Law et al. 2009), including stands of Scots pine (Adams et al. 2011*a*, supplementary information), with values of the function around 0.5 for closely adjacent trees, consistent with the results here. These results point to the importance of local interactions in forest communities, because local gaps for growth are only detected by plants when neighborhoods are small. Further evidence of space-filling comes from the observation that crowns of canopy trees are more regularly spaced than their stems (Gavrikov et al. 1993, Rouvinen and Kuuluvainen 1997, Olesen 2001, Strigul et al. 2008). The space-filling property has the fundamental consequence for plant ecology that area-based ecosystem processes can be uncoupled to some extent from the complexities of organism-based, birth–growth–death processes in plant population and community dynamics.

Our results are consistent with the well-known fact that stand development depends on the initial spatial pattern (e.g., Weiner et al., 2001*a, b*). For instance, we found that plants growing in aggregated spatial patterns had log masses smaller on the average and much more variable in size than those in uniform patterns. Asymmetric competition adds to the variability in size, although our results do not suggest that such competition has priority over spatial pattern (Weiner et al. 2001*b*). The initial size structure was relatively unimportant here, consistent with the observation that early growth in an even-aged stand had less effect on the the stand in the long term than the competition that comes into play when plants are large (Damgaard and Weiner 2008). However, in natural communities, where the initial size structure would include large as well as small plants, the fate of plants would depend more heavily on the space–size organization.

In sum, the methods of spatial-moment dynamics provide ecologists with some useful tools to scale from

microscopic processes of individual plants interacting with neighbors up to the macroscopic dynamics of communities. Creating this bridge enhances ecological understanding in two ways. On one hand, it strips the complexity of algorithmic agent-based models down to a relatively simple mathematical core. On the other hand, it moves mathematical models from a focus on first-order, mean-field approaches that ignore spatial structure, to a focus on second-order approaches that allow spatial structure to unfold over time. There is much ecology to build into local neighborhood interactions, and we would expect the understanding of how plant communities work to be significantly improved by confronting and solving the challenge of scaling up (Levin 2012).

Acknowledgments

The authors acknowledge funding and travel support from the Engineering and Physical Sciences Research Council, Biomathematics and Statistics Scotland and Forest Research (T. Adams), core funding for the Crown Research Institutes from the New Zealand Ministry of Business, Innovation and Employment (P. Holland), the RSNZ Marsden Fund grant number 11-UOC-005 (M. J. Plank, R. Law, T. Adams), an Erskine Fellowship at the University of Canterbury, New Zealand (R. Law), and the Principal's Development Fund and the Mathematics Department at the University of Glasgow (M. Raghib). David Grey suggested the method for obtaining the spatial-moment equations. The research benefited greatly from discussions with Graeme Ackland, Nicholas Hill, and Glenn Marion. We thank two anonymous referees for their comments, which improved and clarified the manuscript.

Literature Cited

Adams, T. P. 2010. Reconstructing Scotland's pine forests. Dissertation. University of Edinburgh, Edinburgh, Scotland, UK.

Adams, T., G. Ackland, G. Marion, and C. Edwards. 2011*a*. Effects of local interaction and dispersal on the dynamics of size-structured populations. Ecological Modelling 222:1414–1422.

Adams, T., G. Ackland, G. Marion, and C. Edwards. 2011*b*. Understanding plantation transformation using a size-structured spatial population model. Forest Ecology and Management 261:799–809.

Adams, T. P., D. W. Purves, and S. W. Pacala. 2007. Understanding height-structured competition: is there an R* for light? Proceedings of the Royal Society B 274:3039–3047.

Barbeito, I., M. Pardos, R. Calama, and I. Canellas. 2008. Effect of stand structure on stone pine (*Pinus pinea* L.) regeneration dynamics. Forestry 81:617–629.

Biging, G. S., and M. Dobbertin. 1992. A comparison of distance-dependent competition measures for height and basal area growth of individual conifer trees. Forest Science 38:695–720.

Biging, G. S., and M. Dobbertin. 1995. Evaluation of competition indices in individual tree growth models. Forest Science 41:360–377.

Bohlman, S., and S. Pacala. 2012. A forest structure model that determines crown layers and partitions growth and mortality rates for landscape-scale applications of tropical forests. Journal of Ecology 100:508–518.

Bolker, B. M., and S. W. Pacala. 1997. Using moment equations to understand stochastically driven spatial pattern formation in ecological systems. Theoretical Population Biology 52:179–197.

Bolker, B. M., S. W. Pacala, and C. Neuhauser. 2003. Spatial dynamics in model plant communities: what do we really know? American Naturalist 162:135–148.

Canham, C. D. 1988. Growth and canopy architecture of shade-tolerant trees: response to canopy gaps. Ecology 69: 786–795.

Canham, C. D., P. T. LePage, and K. D. Coates. 2004. A neighborhood analysis of canopy tree competition: effects of shading versus crowding. Canadian Journal of Forest Research 34:778–787.

Chave, J. 1999. Study of structural, successional and spatial patterns in tropical rain forests using TROLL, a spatially explicit forest model. Ecological Modelling 124:233–254.

Clark, J. S., S. LaDeau, and I. Ibanez. 2004. Fecundity of trees and the colonization–competition hypothesis. Ecological Monographs 74:415–442.

Damgaard, C., and J. Weiner. 2008. Modeling the growth of individuals in crowded plant populations. Journal of Plant Ecology 1:111–116.

Datta, S., G. W. Delius, and R. Law. 2010. A jump-growth model for predator–prey dynamics: derivation and application to marine ecosystems. Bulletin of Mathematical Biology 72:1361–1382.

Dieckmann, U., and R. Law. 2000. Relaxation projections and the method of moments. Pages 412–455 *in* U. Dieckmann, R. Law, and J. A. J. Metz, editors. The geometry of ecological interactions: simplifying spatial complexity. Cambridge University Press, Cambridge, UK.

Gavrikov, V. L., P. Y. Grabarnik, and D. Stoyan. 1993. Trunk–top relations in a Siberian pine forest. Biometrical Journal 35: 487–498.

Gillespie, D. T. 1977. Exact stochastic simulation of coupled chemical reactions. Journal of Physical Chemistry 81:2340–2361.

Gratzer, G., et al. 2004. Spatio-temporal development of forests—current trends in field methods and models. Oikos 107:3–15.

Grimmett, G. R., and D. R. Stirzaker. 2001. Probability and random processes. Oxford University Press, Oxford, UK.

Illian, J., A. Penttinen, H. Stoyan, and D. Stoyan. 2008. Statistical analysis and modelling of spatial point patterns. Wiley, Chichester, UK.

Kendall, D. 1948. On the generalized "birth-and-death" process. Annals of Mathematical Statistics 19:1–15.

Law, R., J. Illian, D. F. R. P. Burslem, G. Gratzer, C. V. S. Gunatilleke, and I. A. U. N. Gunatilleke. 2009. Ecological information from spatial patterns of plants: insights from point process theory. Journal of Ecology 97:616–628.

Law, R., D. J. Murrell, and U. Dieckmann. 2003. Population growth in space and time: spatial logistic equations. Ecology 84:252–262.

Levin, S. A. 2012. Towards the marriage of theory and data. Interface Focus 2:141–143.

Lewontin, R. C. 1974. The genetic basis of evolutionary change. Columbia University Press, New York, New York, USA.

Mason, W. 2000. Silviculture and stand dynamics in Scots pine forest in Great Britain; implications for biodiversity. Investigación agraria. Sistemas y Recursos Forestales 9:175–198.

Murrell, D. J. 2009. On the emergent spatial structure of size-structured populations: when does self-thinning lead to a reduction in clustering? Journal of Ecology 97:256–266.

Murrell, D. J., U. Dieckmann, and R. Law. 2004. On moment closures for population dynamics in continuous space. Journal of Theoretical Biology 229:421–432.

Murrell, D. J., and R. Law. 2003. Heteromyopia and the spatial coexistence of similar competitors. Ecology Letters 6:48–59.

Olesen, T. 2001. Architecture of a cool-temperate rain forest canopy. Ecology 82:2719–2730.

Pacala, S. W., C. D. Canham, J. Saponara, J. A. Silander, R. K. Kobe, and E. Ribbens. 1996. Forest models defined by field

measurements: estimation, error analysis and dynamics. Ecological Monographs 66:1–43.
Penttinen, A., D. Stoyan, and H. M. Henttonen. 1992. Marked point processes in forest statistics. Forest Science 38:806–824.
Pommerening, A. 2002. Approaches to quantifying forest structure. Forestry 75:305–324.
Pommerening, A., V. LeMay, and D. Stoyan. 2011. Model-based analysis of the influence of ecological processes on forest point pattern formation—a case study. Ecological Modelling 222:666–678.
Purves, D. W., and R. Law. 2002. Experimental derivation of functions relating growth of *Arabidopsis thaliana* to neighbour size and distance. Journal of Ecology 90:882–894.
Purves, D. W., J. W. Lichstein, N. Strigul, and S. W. Pacala. 2008. Predicting and understanding forest dynamics using a simple tractable model. Proceedings of the National Academy of Sciences USA 105:17018–17022.
Raghib, M., N. Hill, and U. Dieckmann. 2011. A multiscale maximum entropy moment closure for locally regulated space–time point process models of population dynamics. Journal of Mathematical Biology 62:605–653.
Ribbens, E., J. A. Silander, and S. W. Pacala. 1994. Seedling recruitment in forests: calibrating models to predict patterns of tree seedling dispersion. Ecology 75:1794–1806.
Richards, F. J. 1959. A flexible growth function for empirical use. Journal of Experimental Botany 10:290–300.
Rouvinen, S., and T. Kuuluvainen. 1997. Structure and asymmetry of tree crowns in relation to local competition in a natural mature Scots pine forest. Canadian Journal of Forest Research 27:890–902.
Schneider, M. K., R. Law, and J. B. Illian. 2006. Quantification of neighbourhood-dependent plant growth by Bayesian hierarchical modelling. Journal of Ecology 94:310–321.
Schutz, J. 2002. Silvicultural tools to develop irregular and diverse forest structures. Forestry 75:329–327.
Silvert, W., and T. Platt. 1978. Energy flux in the pelagic ecosystem: a time-dependent equation. Limnology and Oceanography 23:813–816.
Sinko, J. W., and W. Streifer. 1967. A new model for age–size structure of a population. Ecology 48:910–918.
Stoyan, D., and A. Penttinen. 2000. Recent applications of point process methods in forestry statistics. Statistical Science 15:61–78.
Strigul, N., D. Pristinski, D. Purves, J. Dushoff, and S. Pacala. 2008. Scaling from trees to forests: tractable macroscopic equations for forest dynamics. Ecological Monographs 78: 523–545.
Suzuki, S. N., N. Kachi, and J.-I. Suzuki. 2008. Development of a local size hierarchy causes regular spacing of trees in an even-aged *Abies* forest: Analyses using spatial autocorrelation and the mark correlation function. Annals of Botany 102:435–441.
Tautenhahn, S., H. Heilmeier, M. Jung, A. Kahl, J. Kattge, A. Moffat, and C. Wirth. 2012. Beyond distance-invariant survival in inverse recruitment modeling: A case study in Siberian *Pinus sylvestris* forests. Ecological Modelling 233: 90–103.
Taylor, S. L., and D. A. MacLean. 2007. Spatiotemporal patterns of mortality in declining balsam fir and spruce stands. Forest Ecology and Management 253:188–201.
von Foerster, H. 1959. Some remarks on changing populations. Pages 382–407 *in* F. Stohlman, Jr., editor. The kinetics of cellular proliferation. Grune and Stratton, New York, New York, USA.
Weiner, J., and C. Damgaard. 2006. Size-asymmetric competition and size-asymmetric growth in a spatially explicit zone-of-influence model of plant competition. Ecological Research 21:707–712.
Weiner, J., H.-W. Griepentrog, and L. Kristensen. 2001*a*. Suppression of weeds by spring wheat *Triticum aestivum* increases with crop density and spatial uniformity. Journal of Applied Ecology 38:784–790.
Weiner, J., P. Stoll, H. Muller-Landau, and A. Jasentuliyana. 2001*b*. The effects of density, spatial pattern, and competitive symmetry on size variation in simulated plant populations. American Naturalist 158:438–450.
Zeide, B. 1993. Analysis of growth equations. Forest Science 39: 594–616.
Zianis, D., P. Muukkonen, R. Mäkipää, and M. Mencuccini. 2005. Biomass and stem volume equations for tree species in Europe. Silva Fennica Monographs 4:1–63.

Supplemental Material

Appendix

Derivation of the moment approximation for a stochastic birth–death–growth process (*Ecological Archives* E094-253-A1).